THE BELL SYSTEM TECHNICAL JOURNAL
Vol. 61, No. 2, February 1982
Printed in U.S.A.

An Approximate Thermal Model For Outdoor Electronics Cabinets

By J. C. COYNE

(Manuscript received November 18, 1980)

Electronic systems are installed in outdoor loop plant in metal cabinets which are essentially unventilated. The current trend toward greater circuit miniaturization and higher power density increases the difficulty in the thermal design and points up the need for comprehensive thermal design guidelines. As a step toward that end, an approximate lumped thermal-conductance model is presented for calculating steady-state temperatures at three points of the cabinet (the hot sunny wall, the cool shaded wall, and the top row of circuit boards) as functions of input parameters of cabinet geometry, wind speed, solar radiation, and internal heat dissipation (assumed to be uniformly distributed). Calculated results are found to be in agreement with tests within about 10 percent.

I. INTRODUCTION

Electronic systems are typically installed in outdoor loop plant[1] in metal cabinets which are essentially unventilated. The cabinets are subject to ambient temperature excursions from −40 to 120°F and subject to solar heating which can raise the cabinet interior temperatures 30°F above ambient. With a thermal design limit of 185°F at circuit boards, the allowable temperature rise because of circuit dissipation is, thus, limited to about 35°F. The current trend toward greater circuit miniaturization and higher power density further aggravates an already difficult thermal design problem and points up the need for a comprehensive thermal analysis of the outdoor electronic cabinet. This paper is a step in that direction.

The circuit boards are typically arranged in outdoor cabinets (see Fig. 1) in much the same way as in conventional central office equipment bays and, to this extent, the heat transfer mechanisms are similar. In both cases, heat is removed from the circuit boards by

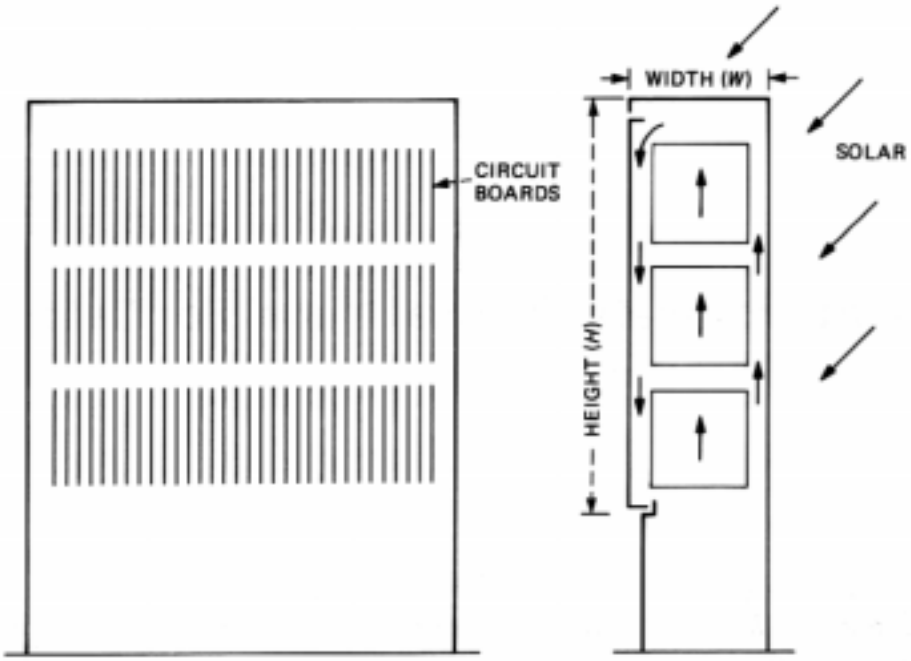

Fig. 1—Convective heat flow in an unventilated electronic cabinet, isolated on one wall.

natural convection; air is warmed by the circuitry and it expands and rises between the columns of boards. But unlike the central office bay situation, the hot air is confined inside the cabinet and must recirculate to transfer its heat to the cabinet walls. In addition, solar heat is absorbed on the sunny exterior cabinet surfaces, some of which is transferred to the cabinet interior and convected to the opposing shaded walls along with the internally dissipated heat. At the exterior surfaces of the cabinet, both solar and dissipated heat are convected and radiated to the ambient.

Whereas, the central office bay problem has been analyzed extensively, very little has been done to date on this more difficult cabinet problem. However, a problem closely related to it, which has received a great deal of study by Elder,[2] Eckert, and Carlson[3] and others, is that of a fluid-filled two-dimensional enclosure whose opposing walls are held at a uniform temperature difference as shown in Fig. 2. This enclosure problem is approximately the same as that of an empty (air-filled) unpowered cabinet in the sun. The main difference is that the walls of the electronic cabinet are not isothermal but, instead, increase in temperature vertically because of natural convection.

The core region of the cabinet of Fig. 1 and the enclosure of Fig. 2 both exhibit a large vertical temperature gradient. According to Elder,[2] the centerline temperature (midway between walls of the enclosure) approaches the hot wall temperature at the top and approaches the cold wall temperature at the bottom, with a gradient at the midway height given by half the difference in wall temperatures divided by the

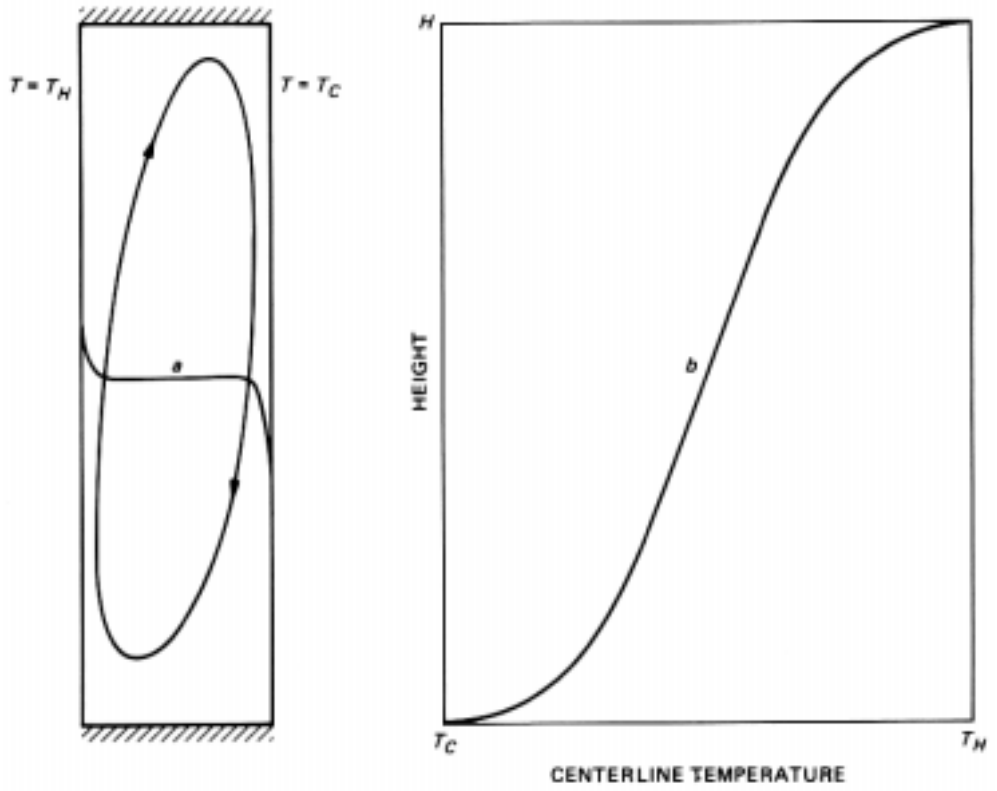

Fig. 2—Two-dimensional enclosure with isothermal side walls, heated at one side, showing flow path and temperature profiles: *a* is horizontal, *b* is vertical.

enclosure height. Laterally, the temperature is nearly constant except near the walls. The vertical gradient violates the isothermal assumption implicit in text-book, heat-transfer relationships for natural convection on vertical walls. As shown later, the error is appreciable.

The enclosure problem shown in Fig. 2 also approximates the convective heat transfer between heat-dissipating circuit boards and the walls of the powered electronic cabinet. The boards can be thought of as the "hot wall" of the enclosure analyzed in the literature. The main assumption here is that the boundary layer flow down the shaded cabinet wall and the heat transfer at this wall is the same regardless of whether the heat originates at an opposing hot wall or at the surface of circuit boards. Using this assumption, heat transfer coefficients from the literature will be incorporated into a simple lumped thermal conductance model from which approximate temperatures can be calculated for a powered electronic cabinet in the sun.

Several empirical relationships for the heat transfer of an enclosure depicted in Fig. 2 have been proposed in the recent literature. For conditions applicable to loop electronic cabinets (Rayleigh number based on height about 10^9, height-to-width ratio about 3, and Prandtl number equal to 0.7) they all are in essential agreement. For instance, Seki et al.[4] in a recent paper propose

$$\mathrm{Nu}_H = 0.36\ \mathrm{Pr}^{0.051} \left(\frac{H}{W}\right)^{-0.11} \mathrm{Ra}_H^{0.25}, \tag{1}$$

where Nu_H = Nusselt number based on enclosure height, Pr = Prandtl number, Ra_H = Rayleigh number based on enclosure height, H = enclosure height and W = enclosure width. After substitution of air properties at 120°F into the dimensionless numbers, Seki's relationship becomes

$$Q = 0.05 A_W W^{0.11} H^{-0.36} (T_H - T_C)^{1.25}, \tag{2}$$

where Q is heat transfer (watts), T_H and T_C are the hot and cold wall temperatures (°F), and A_W is the area (ft^2) of a wall.

Catton[5] recommends the Berkovsky-Polevikov[6] relationship which at 120°F air temperature becomes

$$Q = 0.043 A_W W^{0.09} H^{-0.25} (T_H - T_C)^{1.28}. \tag{3}$$

For typical values of $H = 3$ ft, $W = 1$ ft, and $T_H - T_C = 20$°F, eqs. (2) and (3) agree within 10 percent.

By comparison, the recommended[7] heat transfer relationship for a vertical isothermal plate (assumed to exist in an infinite constant-temperature air space) predicts 23 percent less heat transfer for the same conditions. Thus, the core region in an enclosure, in particular the existence of a vertical temperature gradient in the core, has a significant effect on the heat transfer at the enclosure wall.

For the powered electronic cabinet problem modeled in the next section, eq. (2) will be used as an approximation for the convective heat transfer both between the opposing cabinet walls and between the circuit boards and cabinet walls.

II. A LUMPED THERMAL CONDUCTANCE MODEL

A simple electrical analog for the calculation of approximate steady-state temperatures in a powered electronic cabinet subject to sun and wind is shown on Fig. 3. The absorbed solar radiation, assumed incident on half the cabinet surface, is represented by the heat source Q_s (watts) and the internal heat dissipation by Q_P (watts). Heat is transferred to ambient from the exterior cabinet surfaces by combined long-wave radiation and wind-dependent convection. For radiation, the linearized Stefan-Boltzman equation is used

$$Q_{\mathrm{rad}} = 4\sigma e A_W T_A^3 (T_W - T_A), \tag{4}$$

where σ = Stefan-Boltzman constant (5×10^{-10} watt/ft^2 − °R^4), e = emissivity ($0 < e < 1$), A_W = surface area of one wall (ft^2), T_W = wall temperature (°R), and T_A = ambient temperature (°R).

For the wind-induced heat transfer at the cabinet's exterior surfaces,

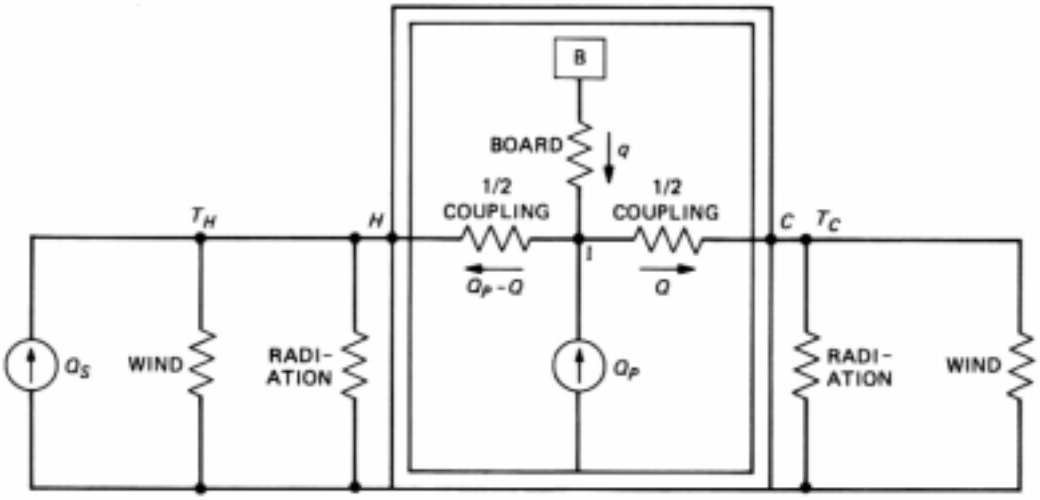

1/2 COUPLING : $Q = 0.119\, W^{0.11} H^{-0.36} A_W (T_I - T_C)^{1.25}$
RADIATION : $Q = 4\sigma A_W T_A^3 (T_C - T_A)$
WIND : $Q = 0.2 (u/D)^{0.5} A_W (T_C - T_A)$
BOARD : $q = hS (T_B - T_I)$

Fig. 3—Lumped conductance model for a powered cabinet in the sun.

consider first the cabinet top. Assume horizontal laminar air flow. The heat transfer (Nusselt number) expressed in terms of Re (Reynolds number) and Pr (Prandtl number) for this situation is given by[8]

$$\mathrm{Nu} = 0.664\ \mathrm{Pr}^{0.33}\mathrm{Re}^{0.5}. \tag{5}$$

Substitution of air properties at 100°F gives

$$h_{\mathrm{wind}} = 0.21(u/D)^{0.5}, \tag{6}$$

where D is the distance across the top measured parallel to the wind direction and u is wind speed (ft/s). For random wind direction, D is approximately given by the average side dimension of the cabinet.

The wind-induced heat transfer at the cabinet's vertical walls at any instant of time depends on the incident wind direction and speed at that time. However, as will be shown, if random wind direction is assumed, then the average heat transfer coefficient (h) at each wall can also be approximated by the simple relationship given in eq. (6). The object here is to preserve the model's simplicity.

Consider the cabinet to be a long square cylinder having side D whose axis is normal to the wind. As before, assume D to be the average side dimension of the cabinet's rectangular cross section. For this situation, the convective heat transfer is given by[9]

$$\mathrm{Nu} = C\ \mathrm{Pr}^{0.35}\mathrm{Re}^{m}, \tag{7}$$

where C and m are constants which depend on wind direction. For a range of Re from 5×10^3 to 10^5, and for the wind normal to a cabinet

wall, $C = 0.1$ and $m = 0.675$. Over the same range of Re, and for the wind direction along a diagonal (45 degrees to a wall), $C = 0.25$ and $m = 0.588$. Assuming random wind direction, the average heat transfer coefficient ($\bar{h}$) is approximately given by the average of these two cases. For a typical case $D = 2$ ft, $u = 5$ ft/s and for air properties at 100°F, $\bar{h}$ is evaluated to be 0.337. The same substitutions into eq. (6) gives $\bar{h} = 0.335$. So, although each wall of the square cylindrical cabinet has a different instantaneous heat-transfer coefficient depending on wind direction, the overall cabinet coefficient is approximately the same as that of a hypothetical cabinet which has wind parallel to all its walls simultaneously. Consequently, with the assumption of random wind direction, the average heat transfer at each cabinet wall is approximately given by

$$Q_{\text{wind}} = 0.21 A_W (u/D)^{0.5} (T_W - T_A). \tag{8}$$

For the internal convective heat transfer from the hot (sunny) cabinet wall to the cool (shaded) cabinet wall, and also from the circuit boards to the cabinet walls, Seki's relationship given in eq. (2) is used. In Fig. 3, this convective coupling is represented by a nonlinear conductance between walls, center-tapped to the heat source Q_P. In adopting Seki's results to the cabinet problem, several differences between the ideal enclosure and the real electronic cabinet are being ignored. The effect of these differences is discussed in Appendix B.

In the no-solar case ($Q_s = 0$ in Fig. 3), Q_P divides equally, half being transferred to each wall. Thus, the temperature at the center tap represents the hottest internal air temperature, which occurs at the top row of electronics if the heat sources are uniformly distributed. Its magnitude relative to the wall temperature is given in the model by half the dissipated power flowing through half the coupling conductance. Thus,

$$T_I - T_W = \frac{R_{\text{coupl}}}{2} \left(\frac{Q_P}{2} \right)^{0.8}. \tag{9}$$

An isothermal board (B) shown in Fig. 3, having an area (two sides) of S ft^2, located in the top row of electronics and dissipating q watts will experience an additional temperature rise above the internal cabinet ambient (center tap) given by

$$T_B - T_I = q/(\text{Sh}), \tag{10}$$

where h is the heat transfer coefficient at the board and S is the board surface area (both sides).

With no internal dissipation ($Q_P = 0$ in Fig. 3), solar heat in the model flows from the hot sunny wall through the coupling conductance to the cool shaded wall. In this case, the temperature at the center-tap

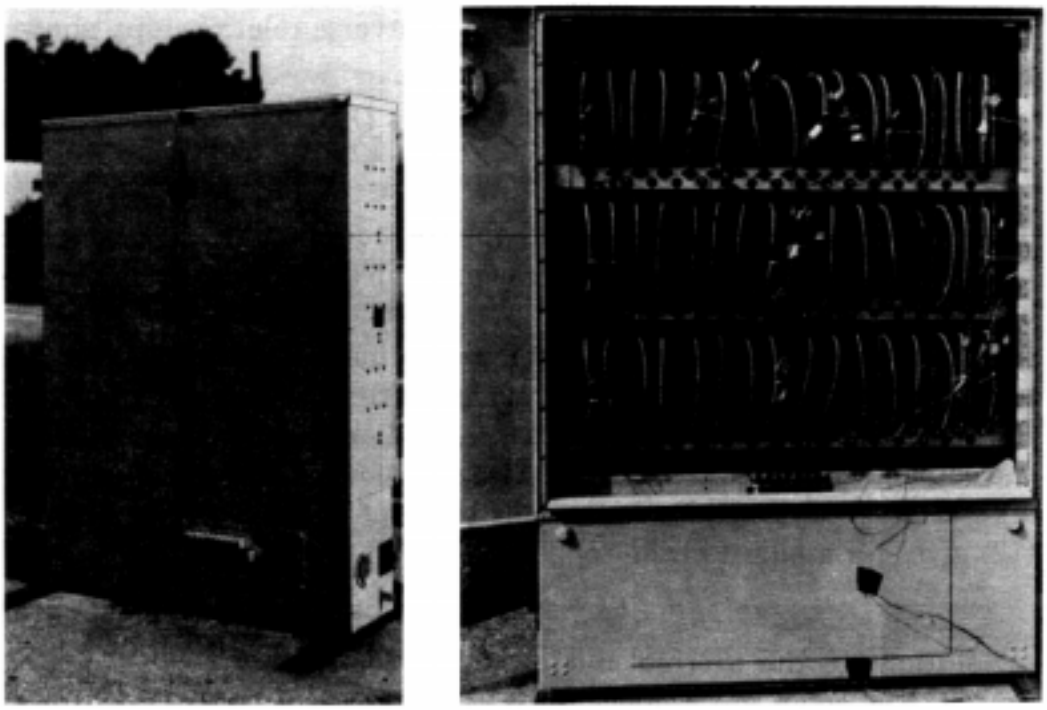

Fig. 4—40E Feeder distribution interface cabinet at test site.

represents the internal temperature at an elevation corresponding to the mean between the hot and cold wall temperatures, which occurs near the midway height of the enclosure in Fig. 2, but somewhat higher in the cabinet of Fig. 1 because of the cabinet wall's vertical temperature gradient.

Thus, in both limiting cases of $Q_P = 0$ or $Q_S = 0$, the proposed thermal conductance model accounts for the flow of heat in roughly the correct way. It remains to be seen how well it agrees with experimental data. For this purpose, the model predictions will be compared with test data taken by the author during the summer of 1979. In these tests, 96 circuit boards, each with eight resistors, were mounted in three rows of *BELLPAC** housings inside a Western Electric 40E FDI cabinet. Figure 4 shows photos of the front and back views of the cabinet at the test site. With all boards powered, the heat dissipation was fairly uniformly distributed in the cabinet.

In evaluating the thermal conductances of the model for this test, assume that the 35 ft^2 surface area of the FDI cabinet is equally divided into 17.5 ft^2 of hot sunny surface and 17.5 ft^2 of cool shaded surface, each at a uniform temperature. In eqs. (2), (4), and (8) substitute $W = 1$ ft, $H = 3.3$ ft, $D = 2$ ft, $u = 10$ ft/s, $T_A = 540°R$, $A_W = 17.5$ ft^2, and $e = 1$ to obtain $Q_{RAD} = 5.51(T_W - T_A)$, $Q_{wind} = 7.86(T_W$

* Trademark of Western Electric Company.

$- T_A)$, and $Q_{coupl} = 0.58(T_H - T_C)^{1.25}$. The inverse relationships, shown on Fig. 5, are

$$T_W - T_A = 0.075(Q_{rad} + Q_{wind}) \tag{11}$$

$$T_H - T_C = 1.54Q_{coupl}^{0.8}. \tag{12}$$

The relationship given by eq. (12) for the coupling conductance has been divided into two series elements in Fig. 5 each having a coefficient of 0.77.

The value of h in eq. (10) was determined experimentally. The measured temperature rise at the center of the board in the middle of the top row relative to the air directly above (about one inch below the cabinet top) gives an effective heat transfer coefficient (h) of about 0.3 watt/ft^2–°F. Substitution of this value of h and $S = 1$ ft^2 into eq. (12) gives for a board in the top row

$$T_B - T_I = 3.3q. \tag{13}$$

Solutions to the thermal model of Fig. 5 for $Q_P = 150$ watts as a function of solar input power are plotted in Fig. 6. To show the sensitivity to wind speed, solutions for both 5 and 10 ft/s winds are presented. Shown on the figure are calculated curves for the cool wall, the hot wall and the top row of boards (points C, H, and B, respectively of Fig. 5). Recognize that the model predicts only a single temperature at each of these locations, whereas in actuality, temperature distributions exist in each case. Experiments were then performed to verify the analytical results at points where the model applies.

III. THERMAL MODEL PREDICTIONS AND COMPARISONS WITH TEST DATA

For purposes of comparing the analytic results with experimental

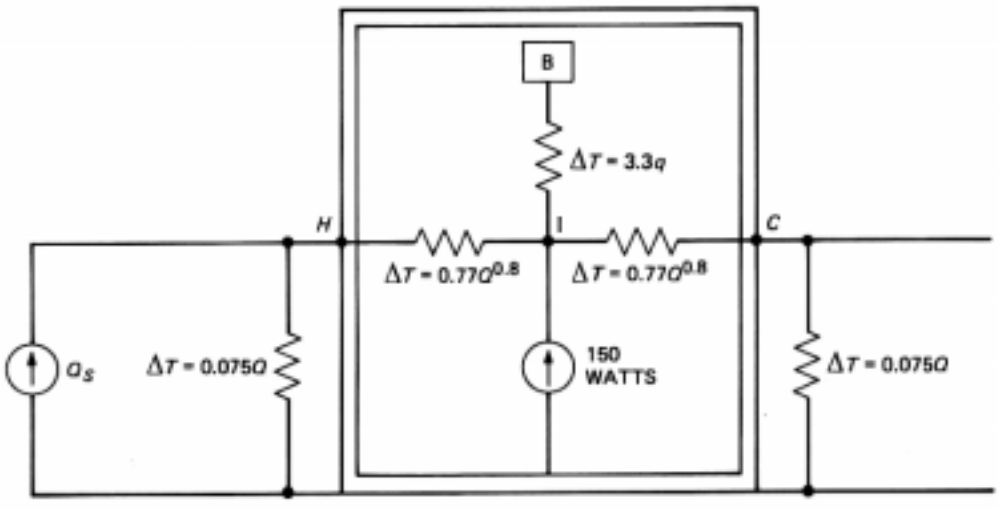

Fig. 5—Lumped conductance model for a powered cabinet in the sun for specific conditions of analysis and tests.

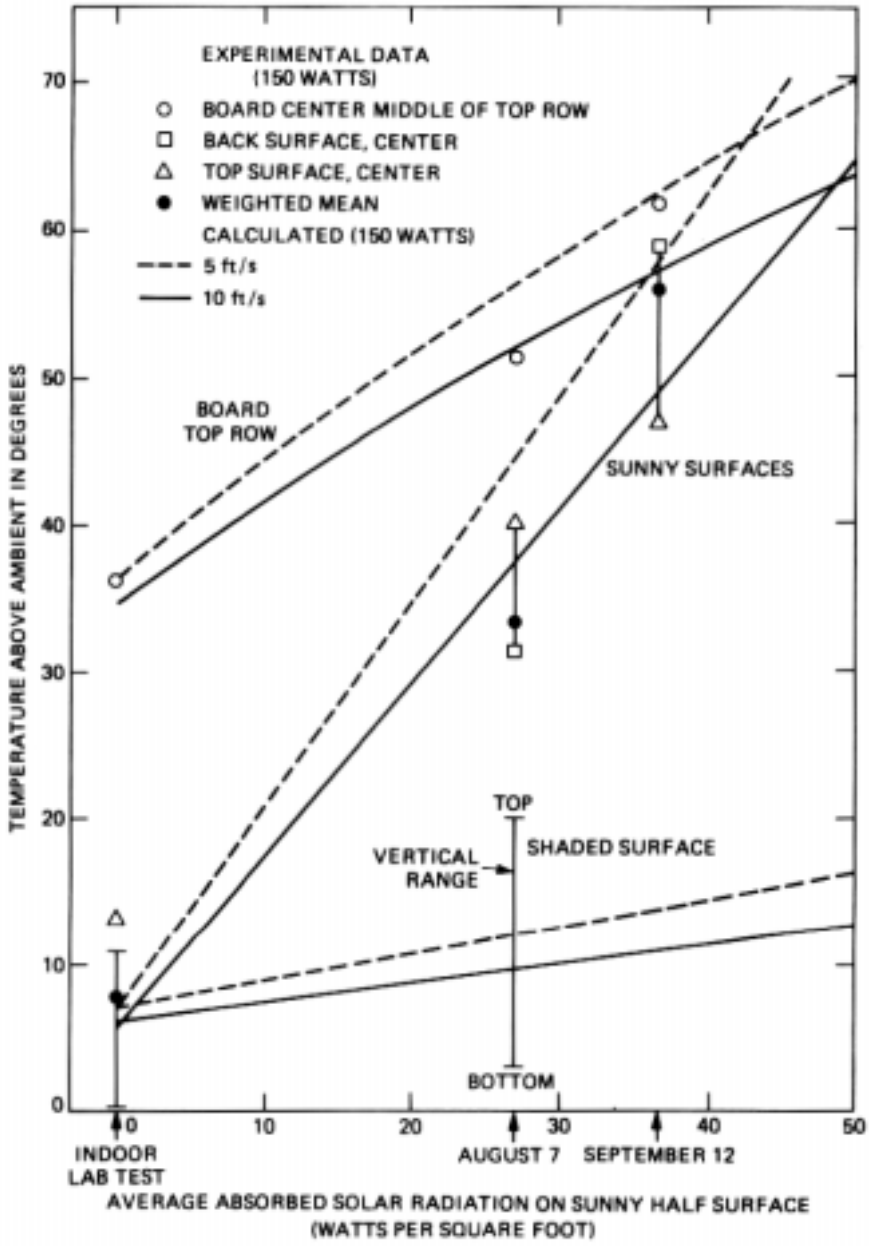

Fig. 6—Measured cabinet temperatures compared with model predictions for Q_p = 150 watts and uniform breeze on all surfaces.

data obtained by the author, two test dates have been selected because of their exceptionally clear skies, August 7 and September 12, 1979. The absence of clouds on these dates simplifies the task of correlating solar intensity with measured cabinet temperatures. Transient effects are small since the cabinet's time constant (measured in the laboratory to be about 0.75 hours) is small compared with the time scale of the solar input waveform. Assuming the solar input to be approximated by a half sine-pulse of 10-hours' duration, the peak daily temperature in the cabinet would be 98 percent of an ideal cabinet having no thermal lag.

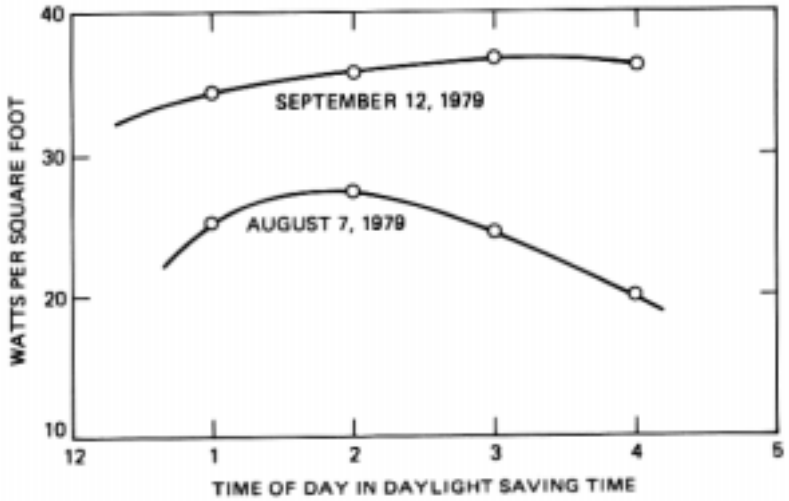

Fig. 7—Average absorbed solar flux calculated from pyranometer traces for two test dates.

Figures 13 and 14 in Appendix A show the incident solar radiation on a horizontal plane for these two dates using a Weatherman R413 star pyranometer. The solar radiation absorbed by the test cabinet for each test date can be calculated from this data. Also needed is a specification of the absorptivity and area of each cabinet surface, as well as the orientation of each surface relative to the direct rays of the sun. This calculation is shown in Appendix A and the results given in Fig. 7.

As shown in Fig. 7, the peak solar power absorbed by the cabinet on September 12 was about 35 percent greater than that on August 7. About half of this large difference was due to the sun's lower position in the sky in September, which resulted in a larger component of direct solar radiation on the cabinet's large back surface. The remaining half was due to a greater solar intensity on September 12, attributable to reduced atmospheric attenuation compared with August 7. As shown in Appendix A, the September 12 intensity equaled the values published by ASHRAE[10] for this date, while the August 7 intensity fell short of ASHRAE values.

Figures 8 and 9 show measured cabinet temperatures for the same two dates. The cabinet top and back surface temperatures, which constitute the sunny hot walls, are plotted versus time of day. Observe that the back surface was hotter than the top surface on September 12, but that the reverse was true on August 7, indicative of the sun's lower altitude in September. The cabinet internal temperature was measured at the center of the board located at the middle of the top row and is believed to be fairly representative of the cabinet's maximum temperature (exclusive of hot spot effects near the resistor heat sources). It is close to the temperature that would occur if the cabinet's

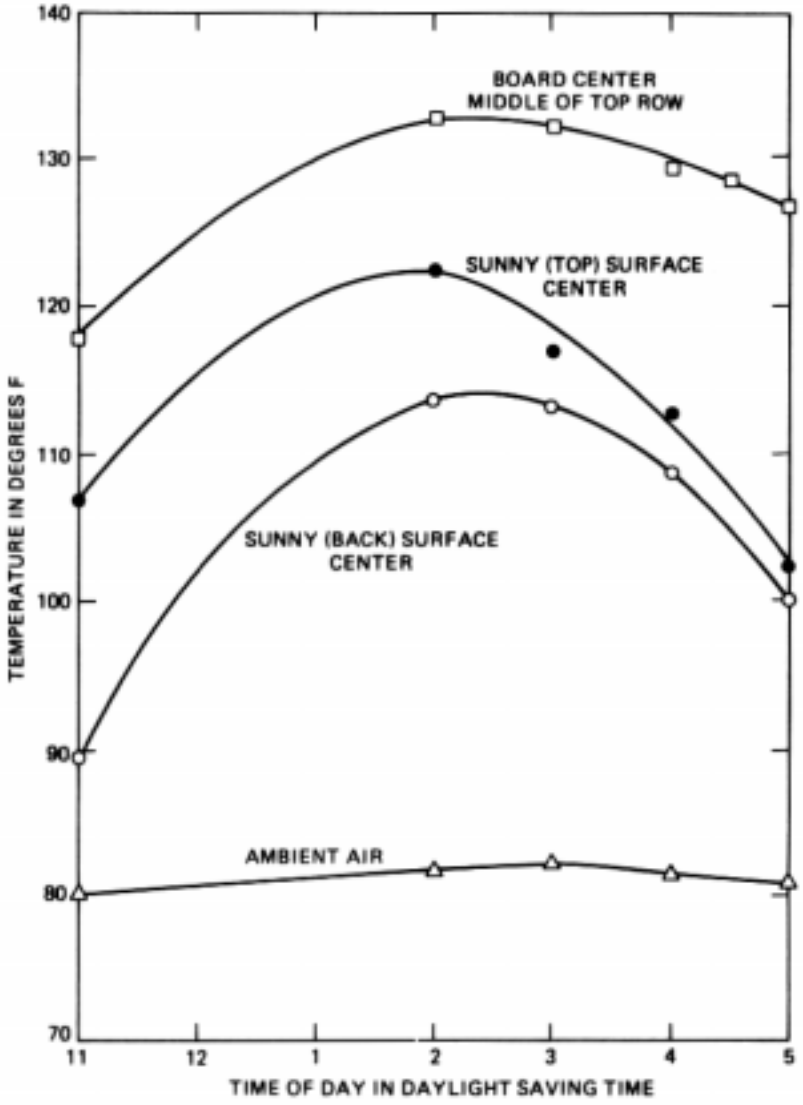

Fig. 8—Cabinet temperatures on August 7, 1979, 150-watt dissipation.

internal dissipation were truly uniform. On September 12 (from Figs. 7 and 9), the cabinet's peak internal temperature rise above ambient was about 62°F; the absorbed solar radiation was 36.5 watts/ft^2. On August 7 (Figs. 7 and 8), the cabinet's peak internal temperature rise was about 51°F; the absorbed solar radiation was 27 watts/ft^2. These results, along with measured surface temperatures, are plotted alongside the analytic results in Fig. 6. Agreement is within 15 percent of the 10 ft/s (6.8 mph) wind curve. The average wind speed during the tests is estimated to be in the range of 5 to 10 mph.

Also given in Fig. 6 is the cool-shaded wall for August 7, shown as a range of temperatures (no measurement made on September 12). It is typical for the shaded wall to have such a vertical temperature gradient since it is the principal heat transfer surface for internal dissipation. By contrast, the sunny hot walls have a fairly uniform temperature.

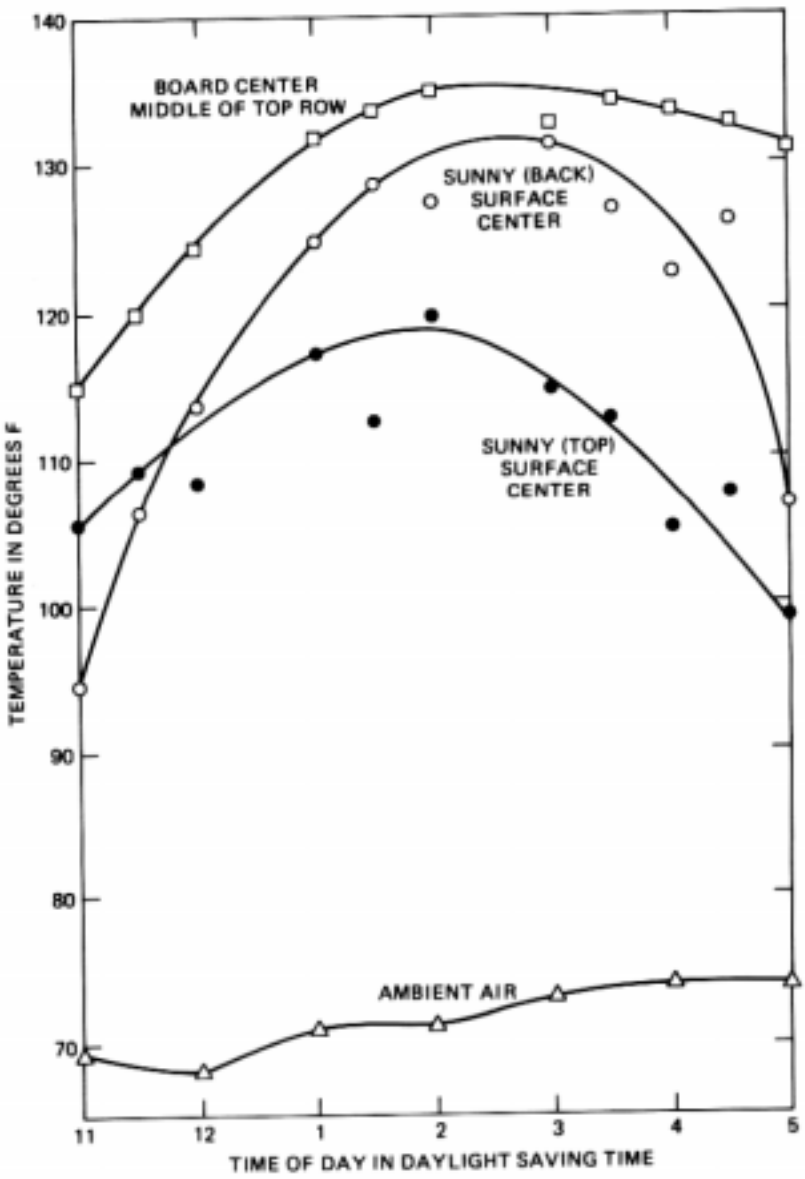

Fig. 9—Cabinet temperatures on September 12, 1979, 150-watt dissipation.

Evidence of this is provided by Fig. 10 which shows vertical temperature profiles measured on the sunny (cabinet back) surface, the shaded (cabinet front) surface and the cabinet centerline (center of boards in the middle of rows). Observe the large vertical temperature gradients on the cabinet center line (1°F/in.) and the shaded surface (0.5°F/in.). By comparison, the sunny surface gradient of 0.1°F/in. is small.

For the case of no solar radiation, Fig. 6 shows experimental temperatures measured in the lab at the same cabinet locations as before. Agreement is almost exact with respect to the 5 ft/s wind curve. The same measurements taken outdoors in the evening or early morning (not shown in the figure) were slightly less because of the action of

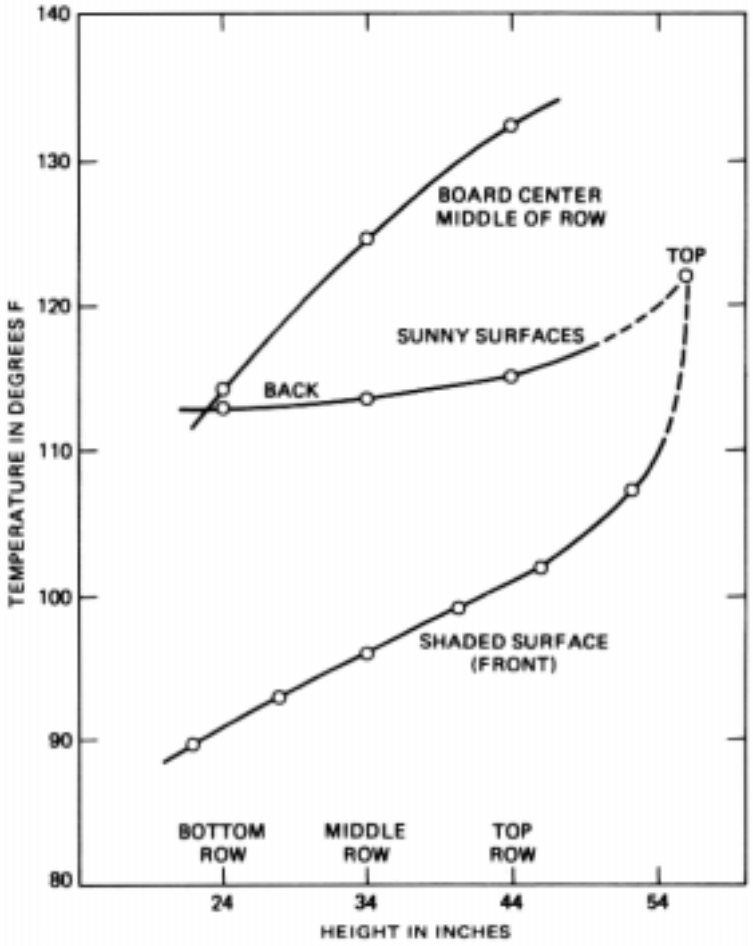

Fig. 10—Vertical temperature profiles on 2 p.m. daylight saving time, August 7, 1979, 150-watt dissipation.

light outdoor breezes. For instance, the board temperature averaged 2 to 3°F cooler, giving closer agreement with the 10 ft/s wind curve.

More generally, for the case of no solar radiation, the model's prediction can be expressed algebraically. From inspection of Fig. 5, the board temperature (T_B) for $Q_S = 0$ and $u = 10$ ft/s is seen to be

$$T_B - T_A = 0.77(Q_P/2)^{0.8} + 0.075(Q_P/2) + 3.3q, \qquad (14)$$

where $q = Q_P/96$. For a 5-ft/s breeze, the 0.075 coefficient becomes 0.106. A comparison of eq. (14) with laboratory experimental temperatures is shown in Fig. 11. The agreement is within 6 percent for both wind speeds over a 250 watt range of Q_P. The calculated curve for wind speed of 5 ft/s is close to lab conditions of natural convection.

Also plotted on Fig. 11 is the measured air temperature (corresponding to T_I in the model) at a point on the cabinet center line about one inch below the cabinet top. The measured temperature rise at the board (T_B) relative to this (T_I) gives the effective heat transfer coefficient of 0.3 watt/ft^2 – °F, which was used to obtain eq. (13).

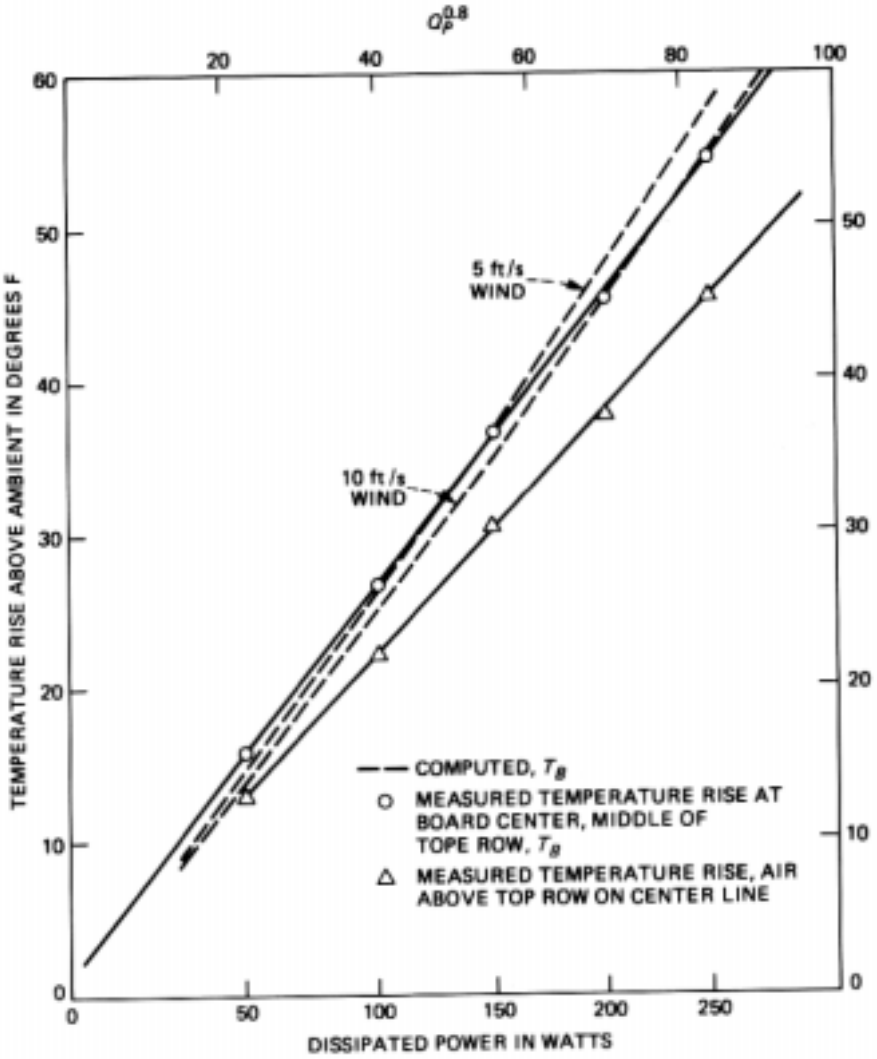

Fig. 11—Comparison of analysis with indoor experimental results.

Returning to Fig. 6, one sees that the measured board temperature agrees fairly well with the analysis for assumed breezes of 5 to 10 ft/s on all cabinet surfaces. Also, the mean hot wall temperature for September 12 (weighted mean of top and back wall) agrees. However, the mean hot wall temperature for August 7 is less than the model prediction. It is believed that the reason for this disagreement is different magnitude breezes on different cabinet surfaces. On August 7, the prevailing breeze direction at the test site was from the south, tending to produce more convective heat transfer at the sunny surfaces than at the shaded surfaces. Figure 12 shows the results of recalculating the cabinet temperatures, increasing the assumed hot wall breeze to 15 ft/s (10.2 mph) and decreasing the assumed shaded wall breeze to 5 ft/s (3.4 mph). The agreement with August 7 data is improved, showing that a reasonable adjustment to the assumed average wind speed at each wall brings the analytic and experimental wall temper-

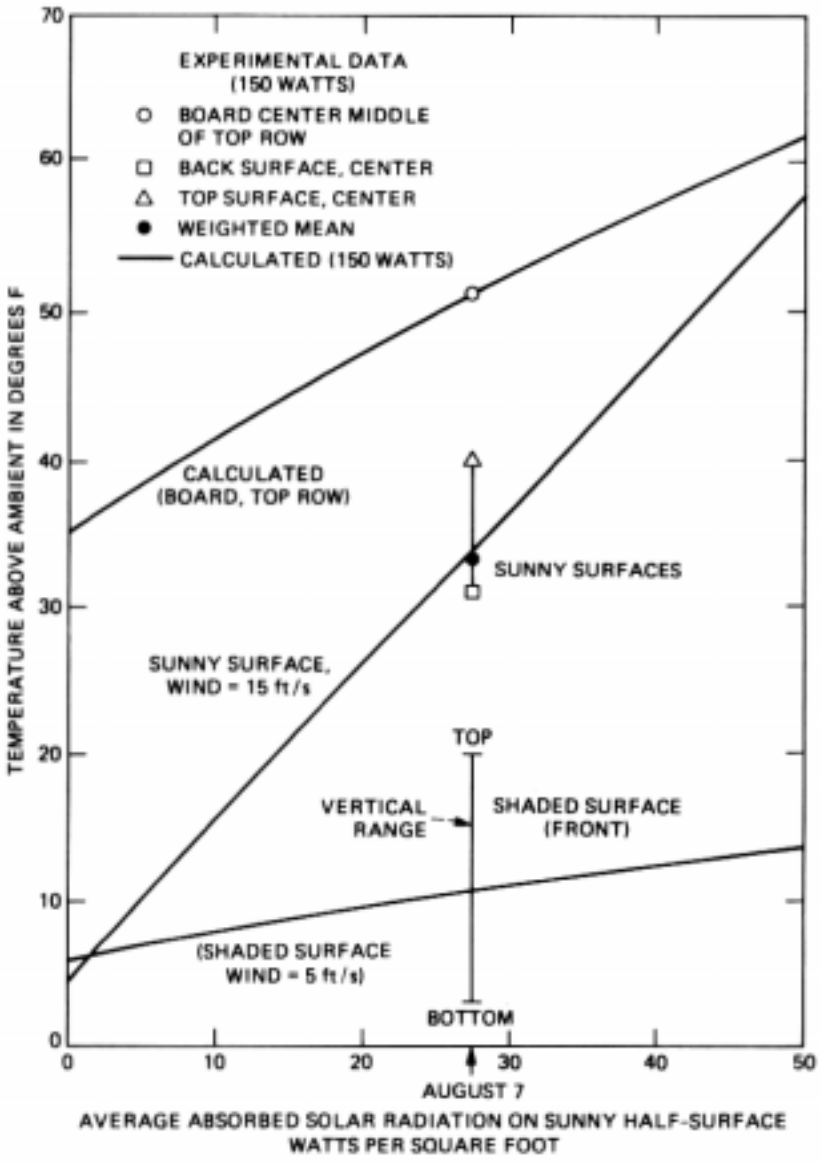

Fig. 12—Measured cabinet temperatures compared with model predictions for Q_p = 150 watts and different wind conditions on opposite cabinet walls.

ature into near perfect agreement. The calculated board temperature is only slightly effected since it depends primarily on average wall conditions.

IV. SUMMARY

An approximate lumped thermal conductance model is presented for calculating maximum steady-state board temperatures in unventilated electronic cabinets, subject to both solar and uniformly-distributed, internally-dissipated heat. The model has general applicability, with input parameters consisting of cabinet geometry, solar radiation, wind speed, and internal heat dissipation.

The main feature of the model is the use of a convective coupling

conductance based on an empirical relationship found in the recent literature for the convective heat transfer between the hot and cold wall of an unpowered enclosure, and the attachment of a heat source (representing internally dissipated heat) to the center tap of this coupling conductance.

Several phenomena are ignored in the analysis. The sensitivity to these are shown in Appendix B to be in the order of 10 percent. Consistent with this, the agreement between the analysis and experimental results is within 10 percent.

The results of this work provides a useful design tool for determining the minimum cabinet size needed to safely dissipate the total heat of a system. The temperature rises of individual devices and circuit boards, which can be determined from individual laboratory tests, can be added to the predicted maximum cabinet ambient (T_I of the model) to give the maximum device or circuit board temperature operating in the full-system cabinet ambient. Also, the analysis tells the designer how much temperature rise to allow for solar radiation and how much cooling can be expected from breezes.

Although useful for predicting the maximum cabinet ambient at the top row, the model does not predict the cooler temperatures at lower rows. This is not a serious limitation for two reasons. First, the thermal design is limited by the maximum temperature which normally occurs at the top. Second, one can determine the vertical temperature profile up between the boards by scaling the results from central office frame analyses. The board temperatures in the cabinet are hotter than in the central office frame because of the reduced convective air flow in the cabinet, but the profiles are similar with respect to height. In both cases, one can assume ambient temperature below the bottom shelf of boards.

A more severe limitation is the model's inability to account for nonuniformly distributed heat sources. A similar difficulty exists in analyzing central office frames where it is common practice to compute temperatures based on average heat dissipation. The cabinet model, by considering just total dissipation, is doing a similar thing. For modest departures from uniformity (e.g., alternate boards powered) the model's effectiveness is unimpaired. Also, certain extremely nonuniform dissipations can be handled. For instance, if all the heat dissipation is at one shelf level, good experimental agreement is obtained if an effective area is substituted into the model which excludes the wall below that shelf level.

These and other topics are under study to refine the approximate model presented here and ultimately to be incorporated into general engineering design guidelines for reliable packaging of loop electronics in outdoor environments.

V. ACKNOWLEDGMENT

The author gratefully acknowledges the encouragement and helpful suggestions given by P. J. Lauriello in the preparation of this paper.

APPENDIX A

Computation of Absorbed Solar Power

Figures 13 and 14 give the vertical component of solar intensity on August 7, 1979, and September 12, 1979, measured by P. E. Fiechter using a Weatherman Star pyranometer. Also shown on each figure are calculated curves of this vertical component using data and relationships given by ASHRAE.[10] Observe that the computed curve of total radiation (direct + diffuse) agrees very well with the September 12 pyranometer trace. By comparison, the pyranometer trace for August 7 falls short of the computed curve for this date. The discrepancy on August 7 is attributed to a light haze on this date.

The total solar power absorbed by the cabinet can be computed from Figs. 13 and 14 and a specification of the orientation of each cabinet wall with respect to the direct rays of sunlight. For this purpose, Fig. 15 shows traces of the sun's altitude angle (L) and azimuth angle (Z) (with respect to south) taken from ASHRAE.[10] The solar power absorbed by each vertical wall is given by

$$Q_V = \alpha A_W I \cos(L)\cos(Z - N)$$

and that absorbed by the top (horizontal) surface

$$Q_H = \alpha A_W I \sin(L),$$

where α is the absorptivity (0.78), N is the angle made by the wall's

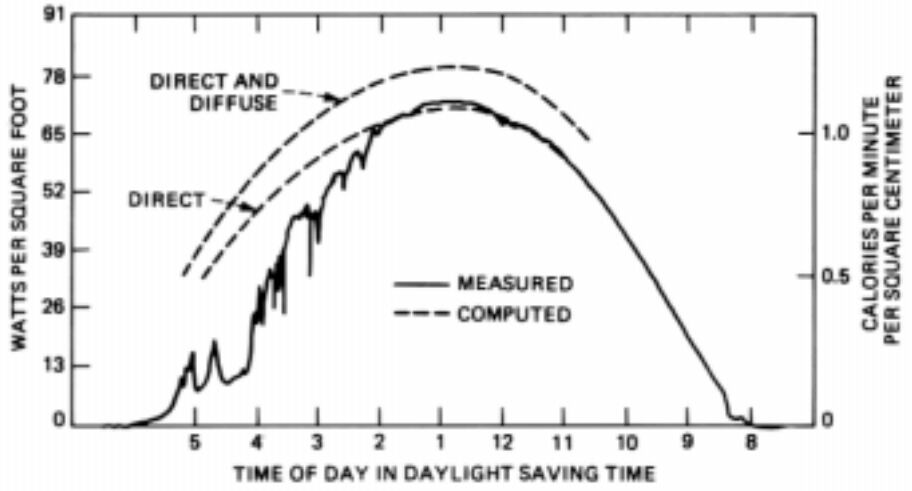

Fig. 13—Pyranometer trace compared with solar intensity computed from ASHRAE data for a horizontal surface on August 7, 1979.

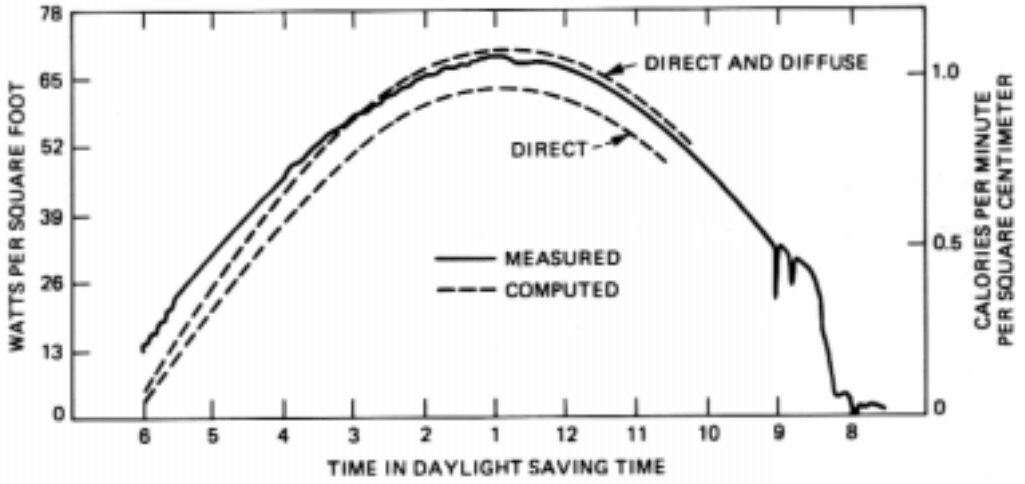

Fig. 14—Pyranometer trace compared with solar intensity computed from ASHRAE data for a horizontal surface on September 12, 1979.

normal with south, A is the wall area (ft^2), and I is the intensity of the direct radiation (watts/ft^2) given by dividing the pyranometer trace by $\sin(L)$. The cabinet surfaces exposed to sun were: top − 3.3 ft^2, side − 3.3 ft^2, back − 11.1 ft^2. The back surface faced 30° west of south ($N = 30°$).

The total absorbed solar power for each date, shown in Fig. 7 of the text, is obtained by adding the contribution of each wall.

APPENDIX B

The Effect of Factors Ignored in the Analysis

Several phenomena which exist in a real electronic cabinet have been ignored in the analysis. This appendix discusses five of these phenomena and estimates their effect on temperature.

In using Seki's results [eq. (1)], the restriction to air flow caused by equipment in the cabinet is ignored. Most of the convected heat is carried in a thin (typically less than one inch) boundary layer at the cabinet walls. The air drag of the equipment, which is mostly in the core of the cabinet, is small provided adequate clearance exists at the walls. The effect on temperatures of this air drag is estimated to be the same order of magnitude as that caused by reducing Seki's enclosure width (W) to a value equal to the sum of the clearances at opposing cabinet walls, say two inches. From eq. (2), one can see that the increase in temperature for an enclosure whose original dimensions are $H = 40$ in. and $W = 10$ in., which is reduced in width to $W = 2$ in., is about 15 percent. Thus, the effect of equipment in the cabinet is estimated to be of the same order of magnitude.

Note that eq. (1) is applicable only within the boundary layer flow-regime which, according to Eckert and Carlson,[3] occurs for height-

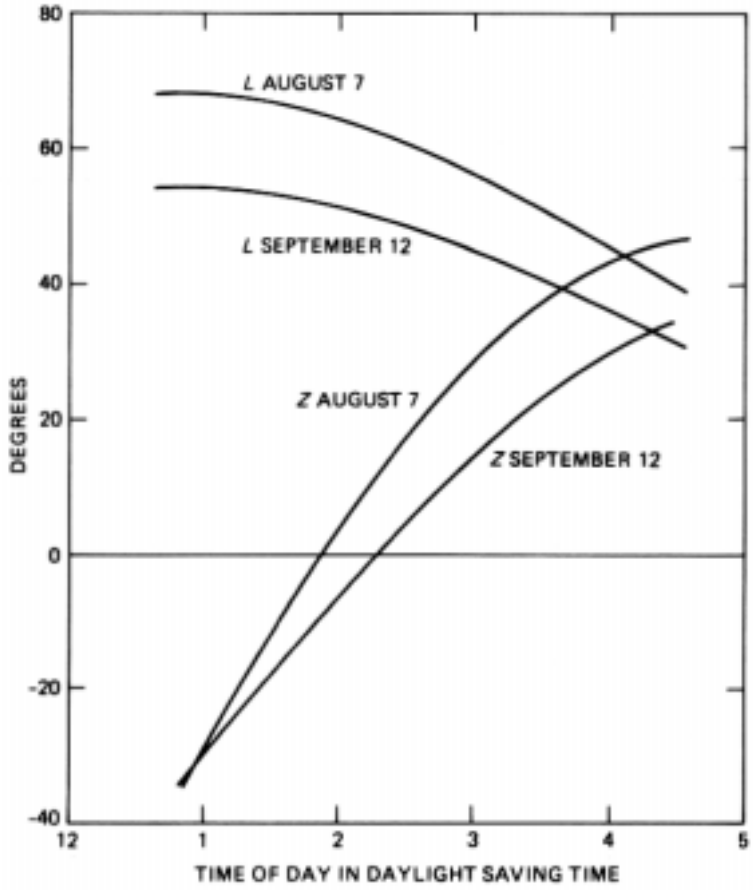

Fig. 15—Solar altitude and azimuth (from south) for test dates.

width ratio less than 2.32×10^{-4} Gr_W, where Gr_W is the Grashof number based on enclosure width. The limiting clearance per wall based on this constraint, for $T_H - T_C = 25°F$ and $H = 40$ in., is 0.9 in. Thus, eq. (2) should be valid for the 1-inch clearance.

A second difference between Seki's enclosure and the real cabinet is the fact that the cabinet walls are not forced to be isothermal. The vertical temperature gradient that naturally occurs up the cabinet walls alters the overall heat transfer from that measured by Seki and others. The effect of this on the internal temperatures is difficult to estimate, but a rough idea can be obtained by comparing the maximum temperature of a constant heat flux wall with that of an isothermal wall, both standing vertically in a uniform ambient. For either wall, $\Delta T = NH^{0.2}Q^{0.8}$, where $N = 8.7$ for constant heat flux and $N = 7.2$ for constant wall temperature. The maximum temperature of the constant heat flux wall is 19 percent greater. Assuming the cabinet walls to lie somewhere between these extremes, then the analysis underestimates the internal cabinet temperatures by about 10 percent.

Conductive and radiative heat transfer have been ignored in the analysis. Conduction from the circuit boards to the cabinet walls is negligible. However, conduction from the hot sunny wall to the cool

shaded wall through the cabinet metal is estimated to be about 0.1 watt/°F for the test cabinet. This conductance amounts to about 10 percent of the convective heat flow given by eq. (2). The average wall temperature and internal cabinet temperature are affected to a much lesser extent.

The heat transfer by radiation from the heat dissipating boards to the cabinet walls depends largely on geometry. For the test conditions consisting of 8-inch deep boards on 1-inch centers, the view factor at the board center is 0.03. Because of this small view factor and because the emissivity of the boards approaches zero in the plane of the board, the heat transfer by radiation is small, calculated to amount to about 10 percent of the boards' dissipation. Consequently, board temperatures are about 10 percent cooler than that predicted by the model.

A fifth factor is the cabinet roof which, in the real cabinet, is a principal heat transfer surface but, in the ideal enclosure, is adiabatic. In the analyses, the roof area was lumped in with that of the vertical walls, thereby assigning to the roof the same average heat transfer as that of the walls. Some error results from the approximation. For instance, in the no-solar case, the heat transfer per unit area through the roof is approximately twice that of the walls (on average), since its temperature equals that at the top (maximum) of walls. Thus, for the test cabinet whose roof comprises 10 percent of the total cabinet surface, the analysis underestimates the total heat transfer and overestimates the cabinet temperature by about 10 percent.

Five factors (more could be added), which are ignored in the analysis, are discussed in this Appendix. Some tend to increase temperature and some decrease temperature. All, broadly speaking, are estimated to have effects in the range of 10 percent. This is consistent with the agreement found between analysis and experiment.

REFERENCES

1. R. W. Henn and D. H. Williamson, "The Loop Plant—Physical Design Considerations," B.S.T.J., *57*, No. 4 (April 1978), pp. 1185–223.
2. J. W. Elder, "Laminar Free Convection in a Vertical Slot," J. Fluid Mech., *23*, Part 1 (1965), pp. 77–98.
3. E. R. G. Eckert and W. O. Carlson, "Natural Convections in an Air Layer Enclosed Between Two Vertical Plates With Different Temperatures," Int. J. Heat Mass Transfer, *2*, (1961), p. 106.
4. N. Seki, S. Fukusako, and H. Inoba, "Visual Observations of Natural Convective Flow in a Narrow Vertical Cavity," J. Fluid Mech., *84*, Part 4, (1978), pp. 695–704.
5. I. Catton, "Natural Convection in Enclosures," Keynote papers of Sixth Int. Heat Transfer Conf., Toronto, *6*, (August 1978) pp. 13–31.
6. D. B. Spalding and H. Afgan, "Heat Transfer and Turbulent Buoyant Convection," *I* and *II*, Washington, DC: Hemisphere Publishing (1977), pp. 443–55.
7. W. H. McAdams, "Heat Transmission," New York: McGraw-Hill 1954, pp. 172–3.
8. H. Grober and S. Erk, "Fundamentals of Heat Transfer," New York: McGraw-Hill, 1961, p. 216.
9. S. S. Kutateladze and V. M. Borishanskii, "A Concise Encyclopedia of Heat Transfer," Elmsford, N. Y.: Pergamon Press, 1966, pp. 140–3.
10. ASHRAE Handbook, American Society of Heating Refrigerating and Air Conditioning Engineers, New York, 1977, pp. 26.1–9.